

SYNTHESIS AND OPTICAL CHARACTERIZATION OF LUMINESCENT ZnO NP's USING *TINOSPORA CRISPA* STEM- A GREEN PERSPECTIVE

U. Nagababu¹, B. Govindh², B. S. Diwakar³, G. Kiran Kumar⁴
And Anindita Chatterjee^{1*}

¹Department of Chemistry, Koneru Lakshmaiah Education Foundation,
Guntur-522502, (Andhra Pradesh) India

²Department of H&S, Raghu Institute of Technology, Visakhapatnam, (Andhra Pradesh) India

³Department of Engineering Chemistry, SRKR Engineering College,
Chinna Amiram, (Andhra Pradesh) India

⁴Department of Physics, Koneru Lakshmaiah Education Foundation,
Guntur, (Andhra Pradesh) India

*E-mail: anindita@kluniversity.in

ABSTRACT

A simple easy and bio-based protocol has been implemented for the synthesis of ZnO Nanoparticle's (NP's) by utilizing the stem of *Tinospora Crispa* plant as a reducing agent. ZnO NP's were probed for both structural and optical characterizations. Optical absorption maxima of the as-synthesized ZnO NP's are observed at 350 nm which indicates the smaller size of the NP's. The XRD study revealed that ZnO NP's are in the wurtzite phase and the average size of the NP's is around 29.1 nm. The shape and size of the NP's are confirmed from TEM. FTIR spectroscopy revealed the surface capping of the NP's by alkaloid moieties present in the *Tinospora Crispa* stem extract. A red shift in optical band gap (3.11 eV) compared with its bulk counterpart (3.37 eV) has been observed. ZnO NP's exhibited excellent photoluminescence properties with a sharp emission maximum at 510 nm due to the oxygen vacancy surface states.

Keywords: Green synthesis, *Tinospora Crispa*, ZnO NP's, X-Ray diffraction (XRD), Fourier transform infrared (FTIR), Photoluminescence (PL)

© RASĀYAN. All rights reserved

INTRODUCTION

Nano-sized colloids exhibit excellent electrical, thermal, optical and catalytic properties¹⁻⁵ as compared to bulk materials. Among the various oxide nanomaterials, ZnO is more preferable as wide band gap (3.37 eV at 300 K) semiconductor material which restrains interesting optical and electrical properties for technological use. ZnO NP's are used in UV light emitters, photocatalyst, as an antibacterial agent, gas sensors, luminescent materials, as an additive in many industries, in solar cell fabrication, heat mirrors and coating.⁶⁻¹⁰ Additionally, ZnO has been subjected to a number of applications in chemistry and in biochemistry.¹¹⁻¹⁹ The reason that among the metal oxide nanoparticles zinc oxide has given much importance is due to its large binding energy, and high piezoelectric property leading to applications in microelectronics, diagnostic and biomolecular detection. Different synthetic methodology has been adopted for preparing ZnO NP's. Conventional techniques explored to obtain ZnO NP's are a chemical reduction, laser ablation, solvothermal, inert gas condensation and sol-gel method.²⁰⁻²⁴ These techniques require toxic chemicals, high pressure, laser radiation and use of inert gases. Alternatively, green synthesis is another technique where the potential of various plants are utilized and shown great interest in the synthesis of zinc oxide NP's²⁵⁻³¹ in a simple, less toxic and cost-effective manner.

Therefore the development of safe, reliable, clean and eco-friendly methods for the preparation of Zinc oxide NP's is essentially needed. Biological methods for the synthesis of ZnO NP's are better methods due to slower kinetics, they offer enhanced manipulation and control over crystal growth and their stabilization. Plant-mediated synthesis of NP's eliminates the cell culture maintaining process and also it is more suitable for large-scale production of ZnO NP's. Keeping all these factors in view, we have prepared the bio-synthesized ZnO NP's from warm water extract of *Tinospora Crispa* plant's stem to make use in photocatalytic, bio-sensing and solar cell applications. The prepared NP's have been characterized by various techniques, like XRD, UV-Visible, Photoluminescence, and FTIR spectroscopy which shows smaller size, good crystallinity, stability and photoluminescence.

EXPERIMENTAL

Chemicals and synthesis

Zinc Acetate (purchased from Himedia chemicals) analytical grade and used as supplied.

Preparation of *Tinospora Crispa*'s Stem Powder Extract

The source plant material was collected locally from Visakhapatnam, India. The stems of this plant were finely cut into pieces and dried at 60^o C keeping inside hot air oven for a span of one week. 100 gm of dried stem powder was taken in a round bottom flask and 200 ml of distilled water was added to it and the mixture was boiled for 30 min and cooled to room temperature. The cooled mixture was centrifuged at 3000 rpm for 10 min. The yellow color supernatant was obtained. It was collected stored and utilized in the second step of the synthesis.

Synthesis of ZnO NP's by Using *Tinospora Crispa* Plant Extract

In the typical biosynthesis of ZnO NP's, 50 ml of plant extract was taken and mixed with 200 ml of Zinc acetate solution of 1mM and stirred at room temperature. The color change in the reaction mixture was observed at first from light yellow to brown before addition of zinc-acetate and thereafter the solution turned into white. The appearance of white color indicates the formation of ZnO NP's by bio-reduction in the completely benign reaction medium. The precipitate of NP's obtained was washed with water and centrifuged at 10,000 rpm for 15 min to remove the impurities and dried to get the powder form of the NP's.

Instrumentation

Synthesized ZnO NP's were first characterized by UV-Visible Spectroscopy by measuring the absorption of the aqueous solution of the as prepared NP's at room temperature using UV-Visible spectrophotometer (Schimadzu UV-Vis Spectrophotometer) between the wavelengths of 300-700 nm. The XRD measurement of ZnO powdered NP's was carried on (XPRT-PRO) XRD setup operated at 40 kV and current 30mA with Cu K α radiation ($\lambda = 1.5404$) and the 2 θ scanning range was 0-90^o at 20 min⁻¹. FTIR studies were performed using Schimadzu FTIR Spectrometer by preparing a sample with KBr pellets and measured at 400 to 4000 cm⁻¹ wavelength range.

TEM was recorded using a high-resolution analytical TEM (Phillips, Netherland Model: Technai20) microscope. For this analysis, the sample was suspended in sterile water & ultrasonically dispersed to separate individual particles & few drops were deposited onto carbon-coated copper grids and dried under an infrared lamp and finally the copper grid was used for scanning.

A fluorescence spectrum was recorded on a Schimadzu Spectrofluorimeter. The optical path was 1 cm and spectra were collected at a resolution of five data points per nanometer. The synthesized ZnO-NP's were dispersed in the aqueous solution to study the photoluminescence activity using an excitation-emission matrix (EEM), which displays fluorescence data.

RESULTS AND DISCUSSION

Characterization of ZnO NP's

The formation of ZnO NP's by reduction of Zinc acetate is observed visibly from the color change observed during synthesis. The plant extract was mixed with Zinc acetate solution and continuously

stirred for 18-24 hours until the color changes from pale brown to white. Figure-1 shows the color change of the plant extract from yellow to brown to white. It provides the confirmation of the reaction between Zinc acetate and plant's stem powder towards the formation of ZnO NP's.

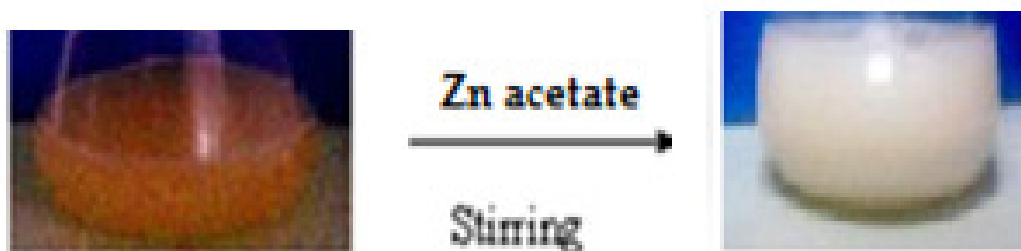


Fig.-1: The Synthesis of ZnO NP's from *Tinospora Crispa* Stem Extract, at First, Color of the Extract changed from Yellow to Light Brown and after 18-24hrs of Stirring the Color of the Solution changed to White.

UV-Visible Spectroscopy

Figure-2a depicts the UV-Visible absorption spectra of ZnO NP's. A smooth and narrow absorption band at 350 nm was observed which is characteristic of small size zinc oxide NP's, as the bulk ZnO absorption peak will appear at 380 nm. The absorption peak shows broadening and slightly moved to the long wavelength region, indicating the formation of ZnO NP's with large size distribution. The position and shape of absorption spectra of ZnO nanoclusters are strongly dependent on the surface-adsorbed species, dielectric medium and particle size.

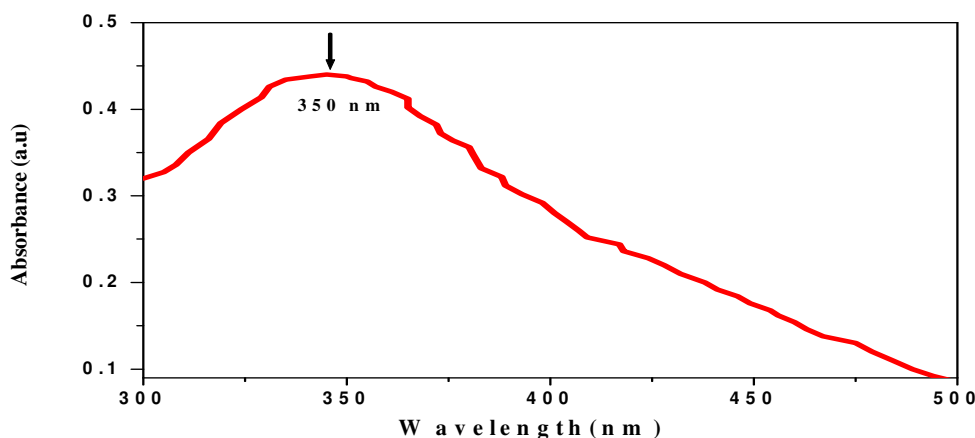


Fig.-2a: UV-Visible Absorption Spectra of ZnO NP's. The Absorption Maxima of ZnO NP's is at 350 nm.

ZnO is a direct band gap semiconductor. Hence, to calculate the band gap energies of ZnO NP's from the absorption edge Tauc equation has been used. The absorption coefficient of the direct band gap material can be written as:

$$(\alpha h\nu)^2 = A (h\nu - E_g) \quad (1)$$

Where, α is absorption coefficient, A is constant, $h\nu$ is photon energy in eV and E_g is direct band gap. The allowed direct band gap could be calculated from the absorbance values by plotting $(\alpha h\nu)^2$ versus $h\nu$, which is shown in Fig.-2b.

The optical band gap determined by extrapolating the linear portion of the Tauc plot (Fig.-2b) to the axis intercepts. The band gap determined to be 3.11 eV which corroborates with the value given in the

literature. The calculation of band gap³² suggested that there is a red shift in optical band gap (3.11eV) compared with its bulk counterpart (3.37 eV).

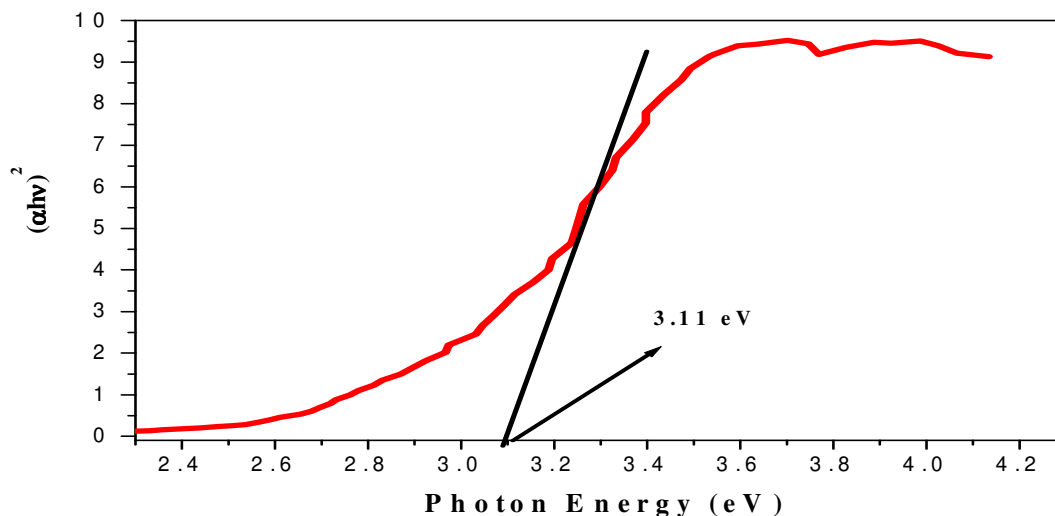


Fig.-2b: Direct Band Gap Studies Using Tauc Equation, by Plotting Optical Absorption Coefficient against Photon Energy of Absorbed by ZnO NP's

TEM

Figure-3 shows the Transmission Electron Microscopy (TEM) image of ZnO NP's. The average grain size of the ZnO NP's was calculated to be around~ 30 nm. The shape of the NP's is hexagonal as observed from a transmission electron microscopic image displayed in Fig.-3. ZnO NP's are scattered over the surface and no aggregates were observed in the TEM image. This indicates NP's are stable however the size distribution of the NP's is broad.

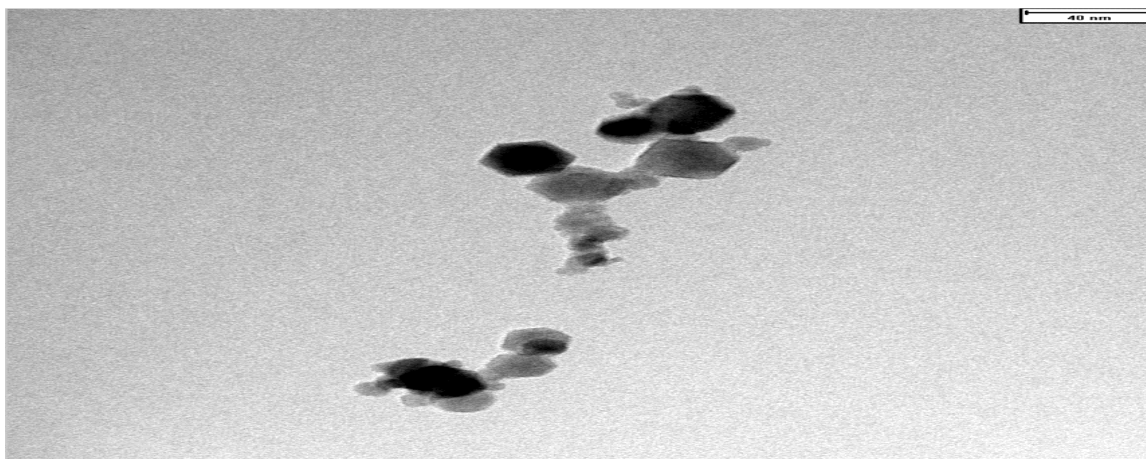


Fig-3: Transmission Electron Microscopic Image of ZnO NP's. The Bar Marker Represents 40 nm.

XRD

Figure-4 shows the XRD pattern of ZnO NP's obtained using *Tinospora Crispa* plant stem extract prepared in the solid powdered state. XRD study revealed that ZnO NP's are in wurtzite³³ phase. The diffraction peaks appeared at $2\theta = 31.78, 34.43, 36.3, 47.54, 56.53,$ and 62.8 which correspond to (100), (002), (101), (102), (110) and (103) planes respectively (JCPDS card (36-451). According to Scherrer's equation, the average crystallite size calculated using the highest peak of 36.3 is found to be 29.1 nm, which is in good agreement with particle size obtained from the TEM image.

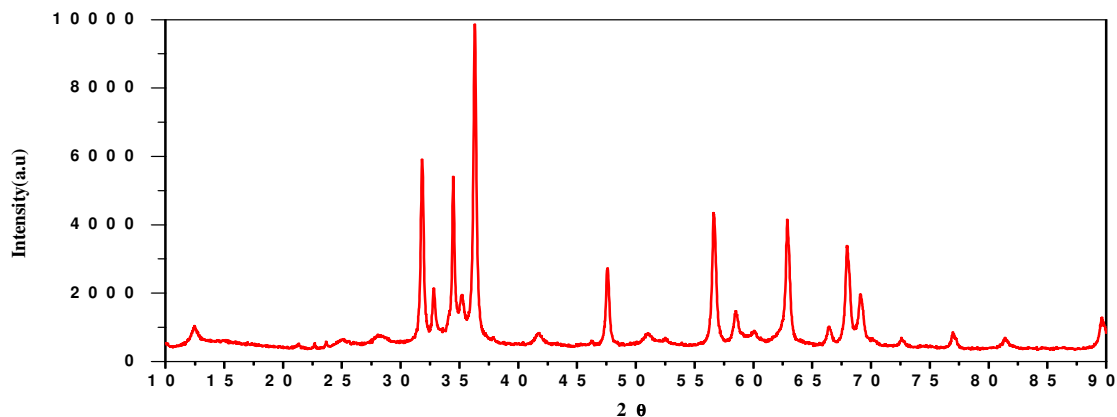


Fig.-4: XRD of ZnO-NP's Synthesized by *Tinospora Crispa* Stem Extract

FTIR Studies

Fourier-transform infrared spectroscopy (FTIR) was carried out to investigate the surface functional groups present in the plant extract which act as a stabilizer in the green synthesis method. FTIR spectra of the green synthesized ZnO NP's has been shown in Fig. 5. The different peaks were observed at different wave numbers such as 3483, 1956-1795, 1372-1250, 1080 cm^{-1} (Fig.-5). The broad peak at 3483 cm^{-1} is due to stretching vibration of hydroxyl groups of alkaloids in the plant extract. The bands observed 1795 cm^{-1} , 1372 cm^{-1} and 1080 cm^{-1} are associated with double bonded carbon, amines and $-\text{C}=\text{O}$ stretching vibrations coming from polysaccharides and reducing sugars present in the plant extract. These show the possible biomolecules responsible for capping & efficient stabilization of the NP's restricting further growth.

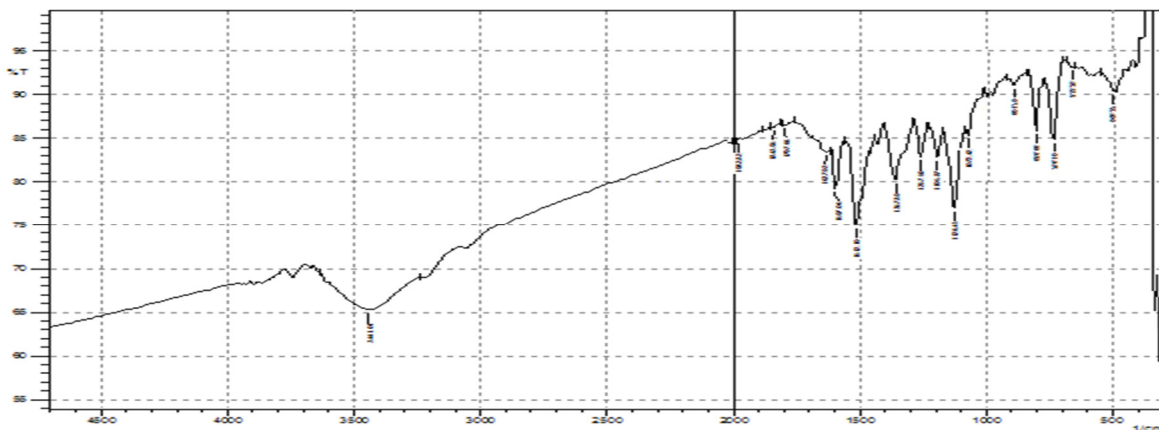


Fig.-5: FT-IR Spectra of *Tinospora Crispa* mediated ZnO NP's.

Photoluminescence Studies

Photoluminescence (PL) of zinc oxide NP's is of prime interest in application point of view of this material. PL is a well-recognized tool for optical characterization of the semiconductor materials for elucidating near band gap emission or defect level emission which may accompany radiative recombination processes. Hypothetically, in pure semiconductors, native defects and defects related to impurities are presently leading to localized defect levels between the band gap. The decay of PL emission Intensity by radiative transitions could be due to the defect levels or near band gap emission. The position and nature of PL spectra give clear idea associated with the transition to identify the specific defects. The Photoluminescence spectroscopic studies carried out at room temperature with our synthesized zinc oxide NP's show emission which is shown in Fig.-6. The sharp luminescence observed in the visible regions (511 nm) is not due to near band gap emission rather associated with intrinsic excitonic defects present in

the grains of the ZnO nanocrystals. To explain the luminescence of ZnO NP's many³⁴ theoretical explanations has been given by many researchers. Luminescence may arise due to the presence of an impurity, or zinc vacancy or oxygen vacancies, interstitial zinc ions etc present in the crystal lattice.³⁵ We propose the emission in green synthesized ZnO NP's is purely due to oxygen vacancy defects. The recombination of a photogenerated hole with the singly ionized charge state of the defects present in the surface of the NP's is responsible for PL emission. This defects might not be passivated by surface capping as no additional stabilized is used in this method. However, the smooth and steady photoluminescence peak observed at 511 nm after excitation at 474 nm makes this bio-synthesized ZnO NP's an interesting and potential material for various luminescent-based applications such as biosensing, photo catalyst and solar cells. The future work in this direction is in progress.

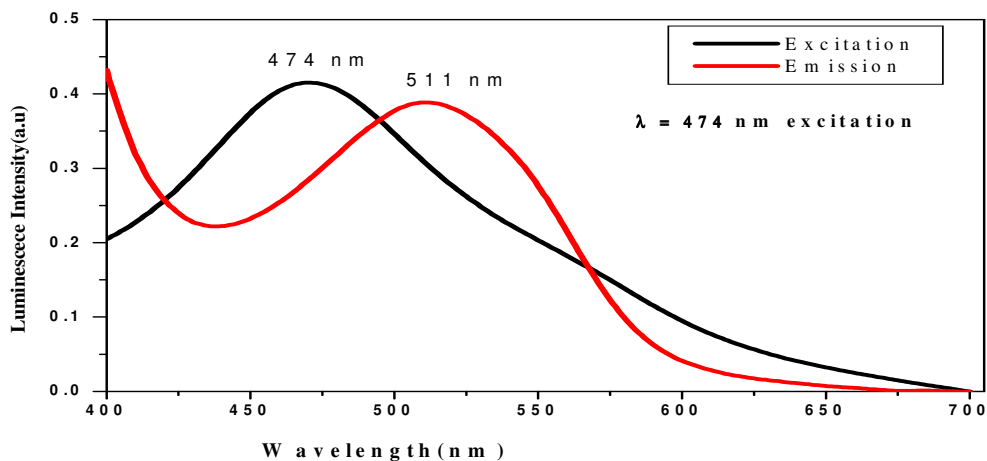


Fig.-6: Photoluminescence Spectra of ZnO NP's. The NP's were excited at 474nm, and Emission Maxima observed at 511 nm.

CONCLUSION

Plant-mediated luminescent ZnO nanoparticles have been synthesized which is simple and easy scale-up process than chemical methods with less toxic chemicals and solvents. Synthesized ZnO nanoparticles were characterized by UV-Vis spectroscopy, TEM, XRD, FTIR, and Photoluminescence spectroscopy. The interesting characteristic of ZnO NP's is that a redshift of optical band gap obtained is 3.11eV which is red-shifted compared to bulk. ZnO NP's exhibit high photoluminescence originated from oxygen vacancies present in the crystal lattice. FTIR spectra provide information of surface capping which is responsible for high photoluminescence. This highly luminescent bio-ZnO NP's could be useful for photocatalytic and solar cell applications.

ACKNOWLEDGMENT

Authors would like to thank management and administration of Koneru Lakshmaiah Education Foundation for their support to carryout this work.

REFERENCES

1. M. A.Hayat, 1989, Colloidal Gold: Principles, Methods and Applications, Academic Press, California.
2. S. Mann, G. A. Ozin, *Nature*, **382**, 313 (1996).
3. G. Cao (ed), 2004, Nanostructures and Nanomaterials: Synthesis, Properties, and Applications. Imperial College Press, London.
4. A. Ingle, A. Gade, S. Pierrat, C. So'nnichsen, M. Rai, *Curr. Nanosci.*, **4**, 141(2008). DOI: [10.2174/157341308784340804](https://doi.org/10.2174/157341308784340804)
5. P. Mukherjee, A. Ahmad, D. Mandal, S. Senapati, S. R. Sainkar, M. I. Khan, R. Parishcha, P. V. Ajaykumar, M. Alam, R. Kumar, M. Sastry, *NanoLett*, **1**, 515 (2001), DOI: [10.1021/nl0155274](https://doi.org/10.1021/nl0155274)

6. H. R. Nawaz, B. A. Solangi, B. Zehra, U. Nadem, *Canadian Journal on Scientific and Industrial Research*, **4**, 164 (2011).
7. H. T. Ng, B. Chen, J. Li, J. Han, M. Meyyappan, J. Wu, SX Li, EE. Haller, *Appl. Phys.Lett.*, **82**, 2023 (2003), DOI: [10.1063/1.1564870](https://doi.org/10.1063/1.1564870)
8. A.Yadav, V. Prasad, A. A. Kathe, S. Raj, D. Yadav, C. Sundaramoorthy, N. Vigneshwaran, *Bull. Matter. Sci.*, **29**, 641 (2006).
9. AAl-Kahlout, *Thin Solid Films*, **520**, 1814 (2012), DOI: [10.1016/j.tsf.2011.08.095](https://doi.org/10.1016/j.tsf.2011.08.095)
10. Q Zhang, C Xie, S Zhang, A Wang, B Zhu, L Wang, Z Yang, *Sens Actuators B*, **110**, 370 (2005), DOI: [10.1016/j.snb.2005.02.017](https://doi.org/10.1016/j.snb.2005.02.017)
11. P. V. Kamat, *J Phys Chem B*, **106**, 7729 (2002), DOI: [10.1021/jp0209289](https://doi.org/10.1021/jp0209289)
12. Haritha Meruvu, Meena Vangalapati, Seema Chaitanya Chippada and Srinivasa Rao Bammidi, *Rasayan Journal of Chemistry*, **4(1)**, 217, (2011).
13. J. R. Lakowicz, *Radiative decay engineering. Anal Biochem*, **298**, 1 (2001), DOI: [10.1006/abio.2001.5377](https://doi.org/10.1006/abio.2001.5377)
14. J. R. Lakowicz, Y. Shen, S. D'Auria, J. Malicka, J. Fang, Z. Gryczynski, I. Gryczynski, *Anal Biochem*, **301**, 261 (2002), DOI: [10.1006/abio.2001.5503](https://doi.org/10.1006/abio.2001.5503)
15. J. R. Lakowicz, *Anal Biochem*, **324**, 153 (2004), DOI: [10.1016/j.ab.2003.09.039](https://doi.org/10.1016/j.ab.2003.09.039)
16. Amrita Raj, Reena Lawrence, *Rasayan Journal of Chemistry*, **11 (3)**, 1339(2018).
17. K. Aslan, I. Gryczynski, J. Malicka, J. R. Lakowicz, C. D. Geddes, *Curr. Opin. Biotechnol*, **16**, 55 (2005), DOI: [10.1016/j.copbio.2005.01.001](https://doi.org/10.1016/j.copbio.2005.01.001)
18. K. Aslan, P. Holley, L. Davies, J. R. Lakowicz, C. D. Geddes, *J Am ChemSoc*, **127**, 12115 (2005), DOI: [10.1021/ja052739k](https://doi.org/10.1021/ja052739k)
19. K. Aslan, S. N. Malyn, C. D. Geddes, *J Fluoresc*, **17**, 7 (2007), DOI: [10.1007/s10895-006-0149-x](https://doi.org/10.1007/s10895-006-0149-x)
20. G. M. Guzmán, J. Dille, S. Godet, *International Journal of Chemical and Biomolecular Engineering*, **2**, 104 (2009).
21. J. M. Cho, J. K. Song, S. M. Park, *Journal of Bull. Korean Chem. Soc.*, **30**, 1616 (2009), DOI: [10.5012/bkcs.2009.30.7.1616](https://doi.org/10.5012/bkcs.2009.30.7.1616)
22. D. Yiamsawas, K. Boonpavanitchakul, W. Kangwansupamonkon, *Journal of Microscopy Society of Thailand*, **23**, 75 (2009).
23. H. Chang, M-H. Tsai, *Journal of Rev. Adv. Mater. Sci.*, **18**, 734 (2008).
24. H. Li, J. Wang, H. Liu, Z. Huaijin, Li Xia, *Journal of Cryst. Growth*, **275**, 943 (2005), DOI: [10.1016/j.jcrysgro.2004.11.098](https://doi.org/10.1016/j.jcrysgro.2004.11.098)
25. A. Ahmad, P. Mukherjee, D. Mandal, S. Senapati, M. I. Khan, R. Kumar, M. Sastry, *J. Am.Chem. Soc.*, **124**, 12108 (2002), DOI: [10.1021/ja027296o](https://doi.org/10.1021/ja027296o)
26. M. Sastry, A. Ahmad, M. I. Khan, R. Kumar, *Curr. Sci.*, **85**, 162 (2003).
27. S. S. Shankar, A. Ahmad, M. Sastry, *Biotechnol. Prog.*, **19**, 1627 (2003), DOI: [10.1021/bp034070w](https://doi.org/10.1021/bp034070w)
28. S. S. Shankar, A. Rai, B. Ankamwar, A. Singh, A. Ahmad, M. Sastry, *Nat. Mater.*, **3**, 482 (2004), DOI: [10.1038/nmat1152](https://doi.org/10.1038/nmat1152)
29. A. Rai, A. Singh, A. Ahmad, M. Sastry, *Langmuir*, **22**, 736 (2006), DOI: [10.1021/la052055q](https://doi.org/10.1021/la052055q)
30. J. L. Gardea-Torresdey, J. G. Parsons, K. Dokken, J. R. Peralta-Videa, H. Troiani, P. Santiago, M. Jose-Yacaman, *Nano Lett.*, **2**, 397 (2002), DOI: [10.1021/nl015673+](https://doi.org/10.1021/nl015673+)
31. J. L. Gardea-Torresdey, E. Gomez, J. R. Peralta-Videa, J. G. Parsons, H. Troiani, M. Jose-Yacaman, *Langmuir*, **19**, 1357 (2003), DOI: [10.1021/la020835i](https://doi.org/10.1021/la020835i)
32. F. K. Shan, G. X. Liu, W. J. Lee, B. C. Shin, *Journal of Crystal Growth*, **291**, 328 (2006), DOI: [10.1016/j.jcrysgro.2006.03.036](https://doi.org/10.1016/j.jcrysgro.2006.03.036)
33. J. S. Ghomi, M. A. Ghasemzadeh, S. Zahedi, *J. MexChem Soc.*, **01**, 01 (2013), DOI: [10.29356/jmcs.v57i1.228](https://doi.org/10.29356/jmcs.v57i1.228)
34. T. Satyanarayana, K. Srinivasa Rao, G. Nagarjuna, *International Scholarly Research Network ISRN Nanotechnology*, (2012), Article ID 372505, DOI: [10.5402/2012/372505](https://doi.org/10.5402/2012/372505)
35. M. Sajjad, I. Ullah, M. I. Khan, J.Khan, M. Y. Khana, Tauseef Qureshi M, *Results in Physics*, **9**, 1301 (2018), DOI: [10.1016/j.rinp.2018.04.010](https://doi.org/10.1016/j.rinp.2018.04.010)

[RJC-4089/2018]